

# A Density Functional Study on the Origin of the Propagation Barrier in the Homogeneous Ethylene Polymerization with Kaminsky-Type Catalysts

John C. W. Lohrenz, Tom K. Woo, and Tom Ziegler\*

Contribution from the Department of Chemistry, University of Calgary,  
2500 University Drive N.W., Calgary, Alberta, Canada T2N 1N4

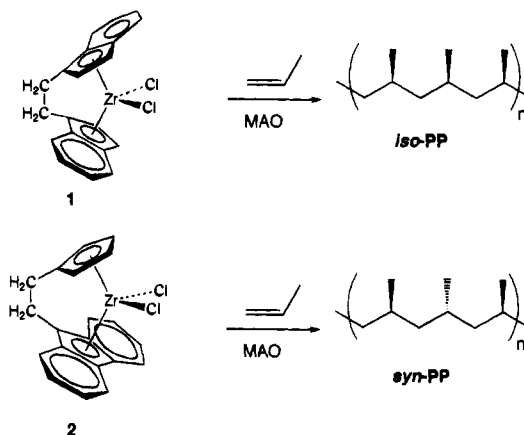
Received June 9, 1995<sup>⊗</sup>

**Abstract:** The reaction of ethylene with  $\text{Cp}_2\text{Zr}^+-\text{Et}$  has been studied with nonlocal density functional theory (DFT). Comparison of four different chain orientations in  $\text{Cp}_2\text{Zr}^+-\text{Bu}$  reveals the high stability of a  $\beta$ -agostic resting state as compared to  $\delta$ - (+30.9 kJ/mol),  $\gamma$ - (+26.9 kJ/mol), and  $\alpha$ -agostic (+46.8 kJ/mol) structures. Thus the  $\beta$ -agostic  $\text{Cp}_2\text{Zr}^+-\text{Et}$  was chosen as the model for the resting state. A  $\beta$ -agostic  $\pi$ -complex is formed in an exothermic reaction ( $\Delta H = -37.1$  kJ/mol). Before insertion can take place, rotation around  $\text{Zr}-\text{C}_\alpha$  has to take place in order to form an  $\alpha$ -agostic intermediate. The electronic barrier for this process amounts to 14.0 kJ/mol and is compensated by a positive entropy of activation ( $\Delta S^\ddagger = +5.5$  J/(mol·K)), a negative change in zero-point energy ( $\Delta H_0 = -10.4$  kJ/mol), and vibrational energy ( $\Delta H_{\text{vib}} = +2.11$  kJ/mol), giving rise to a negligible free energy of activation ( $\Delta G^\ddagger = +0.34$  kJ/mol). After formation of the  $\alpha$ -agostic  $\pi$ -complex the insertion proceeds without any large barriers directly to a  $\beta$ -agostic product via a  $\gamma$ -agostic primary product. The barrier of insertion is 2.0 kJ/mol and barrier for the product reorientation amounts to 2.5 kJ/mol. The overall reaction is exothermic by  $-98.2$  kJ/mol. The propagation barrier corresponds to the rearrangement prior to insertion and rotation takes place in a concerted fashion. H-exchange (chain termination) has a higher electronic barrier ( $\Delta H^\ddagger = +28.2$  kJ/mol), and an only slightly lower free energy of activation ( $\Delta S^\ddagger = -4.5$  J/(mol·K);  $\Delta G^\ddagger = +24.2$  kJ/mol). Rotation is favored over H-exchange because of the high flexibility of the  $\pi$ -complex. This gives a ratio of 15000/1 (insertion/H-exchange) based on Maxwell-Boltzmann statistics. Backside insertion starts with the formation of a backside  $\pi$ -complex and has an activation barrier of 28.4 kJ/mol ( $\Delta S^\ddagger = -16.1$  J/(mol·K),  $\Delta G^\ddagger = +32.5$  kJ/mol).

## I. Introduction

Since the discovery of the titanium chloride catalyzed polymerization of ethylene by Ziegler<sup>1</sup> and the stereoselective polymerization of propene by Natta,<sup>2</sup> many efforts have been undertaken in order to understand the mechanism and the underlying interactions of the Ziegler-Natta polymerization of olefins.<sup>3</sup> This led to the discovery of the homogeneous group-IV metallocene based systems by Kaminsky and co-workers.<sup>4</sup> They found that dichlorozirconocene, when treated with a large excess of methylalumoxane (MAO), is able to catalyze the polymerization of ethylene to high-density polyethylene. Variation of the generic cyclopentadienyl ligands allowed Ewen<sup>5</sup> and almost simultaneously Brintzinger and Kaminsky<sup>6</sup> to produce highly isotactic polypropene from propene using the stereorigid racemic *ansa*-bis(indenyl)zirconium dichloride **1** and MAO. Ewen<sup>7</sup> followed the same strategy and could show that the ethyl-bridged fluorenylcyclopentadienylzirconium catalyst **2** gives syndiotactic polypropene. Apart from this flexibility in the stereoselectivity exhibited by metallocene catalysts many other

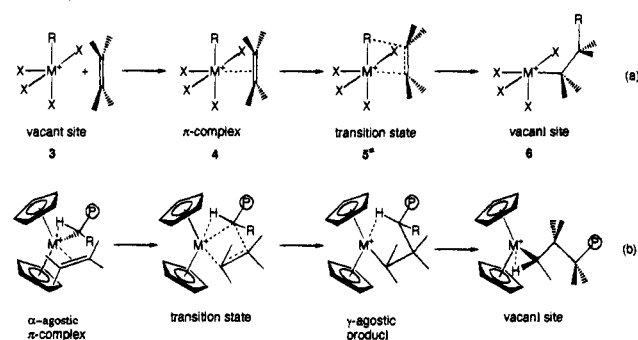
interesting properties such as high activity, a large diversity of the possible ligands, and favorable copolymerization properties, as well as the ability to produce high molecular weight polymers, finally led to their application in industry.



The broad knowledge about the desirable properties stands in contrast to the understanding of the reaction mechanism and the stereoregulating factors in the homogeneous Ziegler-Natta polymerization. From experimental studies by Jordan<sup>8–11</sup> it is known that the active species is cationic and monomeric. It is

<sup>⊗</sup> Abstract published in *Advance ACS Abstracts*, December 1, 1995.  
 (1) Ziegler, K.; Holzcamp, E.; Breil, H.; Martin, H. *Angew. Chem.* **1955**, *67*, 541.  
 (2) Natta, G.; Pino, P.; Corradini, P.; Danusso, F.; Mantica, E.; Mazzanti, G.; Moraglio, G. *J. Am. Chem. Soc.* **1955**, *77*, 1708.  
 (3) Brintzinger, H. H.; Fischer, D.; Müllhaupt, R.; Rieger, B.; Waymouth, R. M. *Angew. Chem., Int. Ed. Engl.* **1995**, *34*, 1143.  
 (4) Andersen, A.; Cordes, H.-G.; Herwig, J.; Kaminsky, W.; Merck, A.; Mottweiler, R.; Pein, J.; Sinn, H.; Vollmer, H.-J. *Angew. Chem., Int. Ed. Engl.* **1976**, *15*, 630.  
 (5) Ewen, J. A. *J. Am. Chem. Soc.* **1984**, *106*, 6355.  
 (6) Kaminsky, W.; Külper, K.; Brintzinger, H. H.; Wild, F. R. W. P. *Angew. Chem., Int. Ed. Engl.* **1985**, *24*, 507.  
 (7) Ewen, J. A.; Jones, R. L.; Razavi, A.; Ferrara, J. D. *J. Am. Chem. Soc.* **1988**, *110*, 6255.

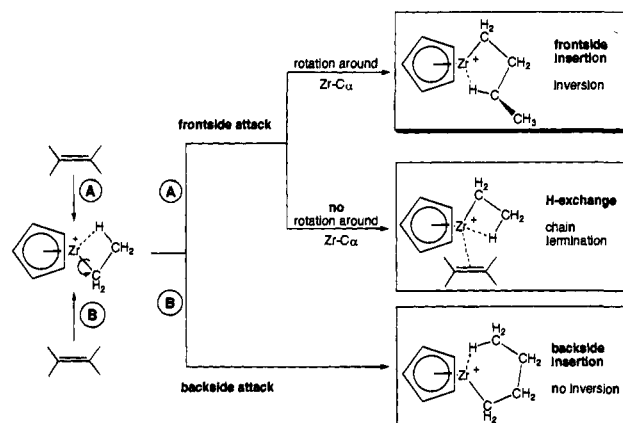
(8) Jordan, R. F. *J. Chem. Educ.* **1988**, *65*, 285.  
 (9) Alelynuas, Y. W.; Jordan, R. F.; Echols, S. F.; Borkowsky, S. L.; Bradley, P. K. *Organometallics* **1991**, *10*, 1406.  
 (10) Gassman, P. G.; Callstrom, M. R. *J. Am. Chem. Soc.* **1987**, *109*, 7875.  
 (11) Jordan, R. F.; Bajgur, C. S.; Willett, R.; Scott, B. *J. Am. Chem. Soc.* **1986**, *108*, 7410.

**Scheme 1** The Cossée–Arlman<sup>12–14</sup> (a) and the Brookhart–Green<sup>15</sup> (b) Mechanism

generally excepted that MAO acts first as a methylating agent and second as the anionic counterion in the reaction. Thus the metallocene has a free coordination site, which is in accordance with the earlier proposed mechanism for heterogeneous systems by Cossée and Arlman<sup>12–14</sup> (Scheme 1a).

The propagation is usually envisioned as follows. In the first step the approaching olefin binds to the vacant coordination site in **3** forming a  $\pi$ -complex **4**. Insertion takes place in a four-membered transition state **5\*** leading to a polymer chain elongated by a  $C_2$ -unit and a new vacant coordination site at the metal **6**, allowing the polymerization to proceed. Brookhart and Green<sup>15</sup> proposed a slightly modified mechanism, assuming that ( $\alpha$ -) agostic interactions play an important role during the reaction (Scheme 1b).

Better understanding of the dominant interactions in the insertion would allow a more directed design of new ligands with superior qualities. In order to accomplish this, over the last years many theoretical investigations<sup>16–39</sup> were carried out, all supporting the Cossée–Arlman or the Brookhart–Green

**Scheme 2** The Reaction of  $Cp_2Zr^+-Et$  with Ethylene: (1) Frontside Insertion; (2) H-Exchange; and (3) Backside Insertion<sup>44</sup>

mechanism. Most studies used a methyl group as a model for the polymer chain and chlorine atoms or cyclopentadienyl rings as ligands. Comparison of the results clearly indicates that Hartree–Fock investigations overestimate the insertion barriers, and that correlated *ab initio* (MP2)<sup>26</sup> and non-local density functional studies<sup>26,36–38</sup> are in good agreement with one another.<sup>39</sup> The calculated low activation barriers for the *insertion* of only 2 to 4 kJ/mol stand in contrast to experimental investigations, which determined *propagation* barriers of 25 to 32 kJ/mol.<sup>40–43</sup>

A recent DFT study by Lohrenz et al.<sup>44</sup> investigated the reaction of the ethylbis(cyclopentadienyl)zirconium cation with ethylene. The authors chose the ethyl group as a model for the resting state between two insertion steps because earlier studies revealed the importance of  $\beta$ -agostic interactions in the products/resting states.<sup>26,36–38</sup> Three different reaction paths were studied (Scheme 2): (1) frontside insertion into the  $\alpha$ -agostic  $\pi$ -complex; (2) hydrogen exchange from the chain end to the complexed olefin (this reaction was shown to be a good model for the chain termination reaction); and (3) insertion into a  $\beta$ -agostic resting state from the backside. The frontside insertion could only be observed when the olefin approached the  $\alpha$ -agostic resting state, which was calculated to be 47 kJ/mol higher in energy than the corresponding  $\beta$ -agostic structure. Since the relative energy of the assumed starting complex was higher than the activation barrier for the chain-terminating H-exchange reaction (+28 kJ/mol), it was concluded that there must be a (concerted) pathway leading from the (most stable)  $\beta$ -agostic  $\pi$ -complex directly to frontside insertion, without rearrangement of the resting state prior to complexation.

We reinvestigated the frontside insertion with the aim to find the proposed reaction path. In the present paper we will describe our results on the complete propagation profile starting from a  $\beta$ -agostic resting state leading to a  $\beta$ -agostic product which can be considered to be the next resting state. The true propagation

- (12) Cossée, P. *J. Catal.* **1964**, *3*, 80.  
 (13) Arlman, E. J. *J. Catal.* **1964**, *3*, 89.  
 (14) Arlman, E. J.; Cossée, P. *J. Catal.* **1964**, *3*, 99.  
 (15) Brookhart, M.; Green, M. L. H. *J. Organomet. Chem.* **1983**, *250*, 395.  
 (16) Armstrong, D. R.; Perkins, P. G.; Stewart, J. J. P. *J. Chem. Soc., Dalton Trans.* **1972**, 1972.  
 (17) Cassoux, P.; Crasnier, F.; Labarre, J.-F. *J. Organomet. Chem.* **1979**, *165*, 303.  
 (18) McKinney, R. J. *J. Chem. Soc., Chem. Commun.* **1980**, 490.  
 (19) Balazs, A. C.; Johnson, K. H. *J. Chem. Phys.* **1982**, *77*, 3148.  
 (20) Shiga, A.; Kawamura, H.; Ebara, T.; Sasaki, T.; Kikuzono, Y. *J. Organomet. Chem.* **1989**, *366*, 95.  
 (21) Proscenc, M.-H.; Janiak, C.; Brintzinger, H.-H. *Organometallics* **1992**, *11*, 4036.  
 (22) Kawamura-Kuribayashi, H.; Koga, N.; Morokuma, K. *J. Am. Chem. Soc.* **1992**, *114*, 8687.  
 (23) Kawamura-Kuribayashi, H.; Koga, N.; Morokuma, K. *J. Am. Chem. Soc.* **1992**, *114*, 2359.  
 (24) Fujimoto, H.; Yamasaki, T.; Mizutani, H.; Koga, N. *J. Am. Chem. Soc.* **1985**, *107*, 6157.  
 (25) Novaro, O.; Blaisten-Barojas, E.; Clementi, E.; Giunchi, G.; Ruiz-Vizcaya, M. E. *J. Chem. Phys.* **1978**, *68*, 2337.  
 (26) Weiss, H.; Ehrig, M.; Ahlrichs, R. *J. Am. Chem. Soc.* **1994**, *116*, 4919.  
 (27) Siegbahn, P. E. M. *Chem. Phys. Lett.* **1993**, *205*, 290.  
 (28) Sakai, S. *J. Phys. Chem.* **1991**, *95*, 7089.  
 (29) Novaro, O. *Int. J. Quantum Chem.* **1992**, *42*, 1047.  
 (30) Meier, R. J.; Dormaele, G. H. J. v.; Iarlori, S.; Buda, F. *J. Am. Chem. Soc.* **1994**, *116*, 7274.  
 (31) Bierwagen, E. P.; Bercaw, J. E.; Goddard, W. A., III *J. Am. Chem. Soc.* **1994**, *116*, 1481.  
 (32) Castonguay, L. A.; Rappé, A. K. *J. Am. Chem. Soc.* **1992**, *114*, 5832.  
 (33) Jolly, C. A.; Marynick, D. S. *J. Am. Chem. Soc.* **1989**, *111*, 7968.  
 (34) Yoshida, T.; Koga, N.; Morokuma, K. *Organometallics* **1995**, *14*, 746.  
 (35) Fan, L.; Harrison, D.; Deng, L.; Woo, T. K.; Swerhone, D.; Ziegler, T. *Can. J. Chem.* **1995**, *73*, 989.  
 (36) Fan, L.; Harrison, D.; Woo, T. K.; Ziegler, T. *Organometallics* **1995**, *14*, 2018.

- (37) Woo, T. K.; Fan, L.; Ziegler, T. In *40 Year Ziegler-Catalyses*; Freiburg/Breisgau, Germany, 1993.  
 (38) Woo, T. K.; Fan, L.; Ziegler, T. *Organometallics* **1994**, *13*, 2252.  
 (39) Axe, F. U.; Coffin, J. M. *J. Phys. Chem.* **1994**, *98*, 2567.  
 (40) Chien, J. C. W.; Razavi, A. *J. Polym. Sci. Part A: Polym. Chem.* **1988**, *26*, 2369.  
 (41) Chien, J. C. W.; Bor-Ping Wang. *J. Polym. Sci. Part A: Polym. Chem.* **1990**, *28*, 15.  
 (42) Chien, J. C. W.; Tasai, W.-M.; Rausch, M. D. *J. Am. Chem. Soc.* **1991**, *113*, 8570.  
 (43) Chien, J. C. W.; Sugimoto, R. *J. Polym. Sci. Part A: Polym. Chem.* **1991**, *29*, 459.  
 (44) Lohrenz, J. C. W.; Woo, T. K.; Fan, L.; Ziegler, T. *J. Organomet. Chem.* **1995**, *497*, 91.

barrier will be presented and a comparison with already published alternative reaction paths will follow.

## II. Computational Details

The present density functional investigation used the program system ADF1.1.3, developed by Baerends *et al.*<sup>45</sup> The program was vectorized by Ravenek.<sup>46</sup> Velde *et al.*<sup>47,48</sup> developed the numerical integration procedure which was used for the calculations. The geometry optimization scheme was based on a method implemented by Verluis and Ziegler.<sup>49</sup>

For the description of the electronic configuration (4s, 4p, 4d, 5s, and 5p) of zirconium we used an uncontracted triple- $\zeta$  STO basis set.<sup>50,51</sup> For carbon (2s, 2p) and hydrogen (1s) a double- $\zeta$  STO basis,<sup>50,51</sup> augmented with a single 3d or 2p polarization function, respectively, was applied. No polarization functions were employed for carbons and hydrogens on the Cp ring. The core (1s<sup>2</sup>2s<sup>2</sup>2p<sup>6</sup>3s<sup>2</sup>3p<sup>6</sup>3d<sup>10</sup> on Zr; 1s<sup>2</sup> on C) was treated by the frozen core approximation.<sup>52</sup>

In order to fit the molecular density and represent Coulomb and exchange potentials accurately a set of auxiliary s, p, d, f, and g STO functions,<sup>53</sup> centered on all nuclei, was used in every SCF cycle.

Energy differences were calculated by including the local exchange correlation potential by Vosko *et al.*<sup>54</sup> with Becke's<sup>55</sup> non-local exchange and Perdew's<sup>56</sup> non-local correlation (NL) corrections. The optimizations were carried out at the local level (LDA) of theory.

Local C<sub>5</sub> symmetry was assumed for the Cp rings in the optimizations. No other constraints were applied. The transition states were located according to the following procedure: First all variables but the reaction coordinate were optimized and the reaction coordinate was stepwise varied. The maximum of this linear transit served as the starting structure in a transition state search, now without any geometry constraints except for those mentioned earlier. All transition states shown are true transition states at the local level of theory as proven by exactly one imaginary frequency, except for the transition state for the frontside insertion, which does not show an imaginary frequency at the LDA geometry.

The calculation of the thermodynamic data followed standard textbook procedures.<sup>57</sup> In the frequency calculations the Cp rings were treated as rigid and only the center of mass was displaced. We assume that the frequencies within the Cp rings are unlikely to change considerably during the reaction. The zero-point energy as well as the change in vibrational entropy and enthalpy did not consider the imaginary frequencies in the transition states.

## III. Propagation

In this section we wish to present our recent calculations together with the earlier published<sup>44</sup> results on the insertion reaction of ethylene into the ethylbis(cyclopentadienyl)zirconium cation. In the beginning we shall comment on the nature of the resting state between two insertion steps: four possible chain orientations will be compared and a case will be made for the ethyl group being a good model for the polymer chain.

(45) ADF 1.1.3, Baerends, E. J., 1995, Vrije Universiteit Amsterdam.

(46) Ravenek, W. In *Algorithms and Applications on Vector and Parallel Computers*; Riele, H. J. J. t., Dekker, T. J., Vorst, H. A. v. d., Eds.; Elsevier: Amsterdam, 1987.

(47) Boerrigter, P. M.; Velde, G. t.; Baerends, E. J. *Int. J. Quantum Chem.* **1988**, *33*, 87.

(48) Velde, G. t.; Baerends, E. J. *J. Comput. Phys.* **1992**, *99*, 84.

(49) Versluis, L.; Ziegler, T. *J. Chem. Phys.* **1988**, *88*, 322.

(50) Snijders, J. G.; Vernooijs, P.; Baerends, E. J. *At. Nucl. Data Tables* **1981**, *26*, 483.

(51) Vernooijs, P.; Snijders, G. J.; Baerends, E. J. *Slater Type Basis Functions for the whole Periodic System*; Free University of Amsterdam, The Netherlands, 1981.

(52) Baerends, E. J. Ph.D. Thesis Thesis, Vrije Universiteit, 1975.

(53) Krijn, J.; Baerends, E. J. *Fit Functions in the HFS-method*; Free University of Amsterdam, The Netherlands, 1984.

(54) Vosko, S. H.; Wilk, L.; Nusair, M. *Can. J. Phys.* **1980**, *58*, 1200.

(55) Becke, A. D. *Phys. Rev.* **1988**, *A38*, 3098.

(56) Perdew, J. P. *Phys. Rev.* **1986**, *B33*, 8822; **1986**, *B34*, 7406.

(57) McQuarrie, D. A. *Statistical Thermodynamics*; Harper & Row: New York, 1973.

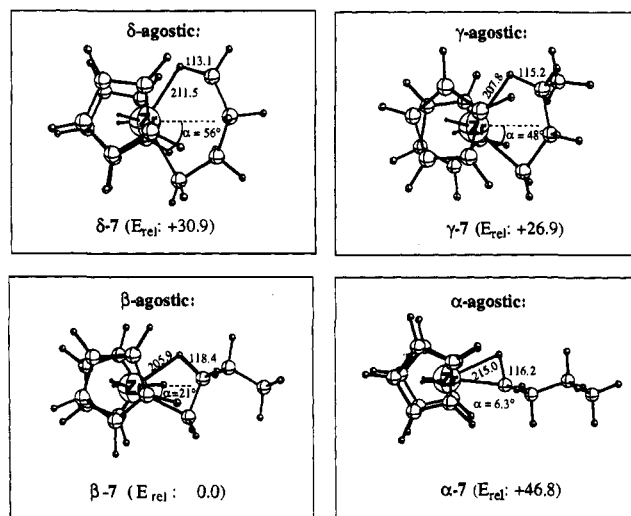


**Figure 1.** Orientations of the butyl chain in  $Cp_2Zr^+-Bu$ ; relative energies in kJ/mol, distances in pm, angles in deg.  $\alpha$  is the out-of-plane angle of the  $\alpha$ -carbon atom with respect to the centroid-Zr-centroid plane.

Subsequently the reaction profile will be discussed in detail. The propagation will be presented in three separate steps: (i) rearrangement of the  $\beta$ -agostic to an  $\alpha$ -agostic  $\pi$ -complex; (ii) insertion of the olefin and C-C bond formation; and (iii) rearrangement of the primary  $\gamma$ -agostic product to the most stable  $\beta$ -agostic resting state.

At the end of this section we will compare our findings with the earlier discussed chain termination reaction via H-exchange and the alternative insertion from the backside.

**The Structure of the Resting State.** All high-level quantum mechanical investigations on the mechanism of the Ziegler-Natta polymerization revealed the importance of agostic interactions in the course of the reaction.<sup>22-24,26,28,30,32,34,36-38,44</sup> More recent studies agree on the fact that the most stable conformation of the (modeled) polymer chain contains a  $\beta$ -agostic interaction. This structure has been calculated to be between 11 and 25 kJ/mol more stable than an alternative  $\gamma$ -agostic conformation.<sup>26,34,36-38,44</sup>

In Figure 1 four possible orientations of the alkyl chain in the butylbis(cyclopentadienyl)zirconium cation are shown together with the relative energies. The most stable structure is the  $\beta$ -agostic  $\beta$ -7 with the shortest Zr-H distance (205.9 pm) and the longest C-H bond (118.9 pm) of all studied conformers.  $\beta$ -7 is 30.9 kJ/mol more stable than the  $\delta$ -agostic  $\delta$ -7. Here, the Zr-H distance is much larger (211.5 pm) and the C-H bond shorter (113.9 pm), i.e. the agostic interaction is weaker and the stabilizing effect is reduced. Another reason for the high relative energy of  $\delta$ -7 might be an unfavorable steric repulsion of the  $\delta$ -methyl as well as the  $\alpha$ -methylene group with the cyclopentadienyl ligands. In  $\delta$ -7 the angle  $\alpha$  describing the position of the  $\alpha$ -methylene group with respect to the centroid-Zr-centroid plane is very large (56° in  $\delta$ -7 vs 21° in  $\beta$ -7). The larger the angle  $\alpha$ , the closer the methylene protons are to the Cp rings.  $\gamma$ -7 is slightly more stable than  $\delta$ -7 (-4.0 kJ/mol), but still strongly destabilized if compared to  $\beta$ -7 ( $E_{rel} = +26.9$  kJ/mol). The  $\gamma$ -agostic interaction is stronger (Zr-H = 207.8 pm; C-H = 115.2 pm) and steric interactions are reduced ( $\alpha = 48^\circ$ ) in  $\gamma$ -7 when compared to  $\delta$ -7. Remarkably, the least stable conformer is the  $\alpha$ -agostic  $\alpha$ -7 (+46.8 kJ/mol), most likely due to a weaker agostic interaction (Zr-H = 216.5 pm; C-H = 116.1 pm; Zr-C-H: 73.1°) as well as an unfavorable steric interaction of the ligands with the polymer chain, which is pointing out of the plane. The interaction is weakened by a

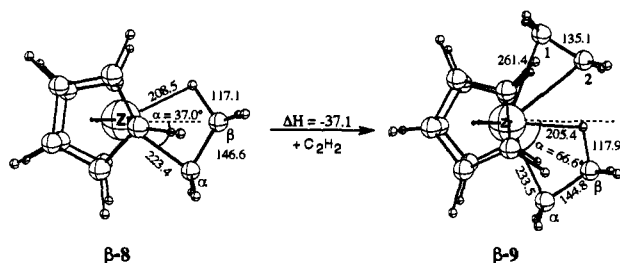


**Figure 2.** Formation of the  $\beta$ -agostic  $\pi$ -complex  $\beta$ -9 from the resting state  $\beta$ -8; energy in kJ/mol, distances in pm, and angles in deg.  $\alpha$  is the out-of-plane angle of the  $\alpha$ -carbon atom with respect to the centroid-Zr-centroid plane.

large Zr-C $\alpha$ -C $\beta$  angle of 136.2°. A reason for the weak agostic interaction is the high ring strain induced by the formation of a three-membered ring. At the same time the overlap of the empty zirconium d-orbital with the C-H bond is difficult.

It can be assumed that the chain end will remain in a  $\beta$ -agostic orientation between two insertions and that a reorientation to an  $\alpha$ -agostic structure prior to olefin complexation is very unlikely. Thus, frontside insertion will begin with an attack of the olefin at the  $\beta$ -agostic complex. This makes it necessary to choose at least an ethylzirconocene cation as the model for the active catalyst. The results of its reaction with ethylene are presented in the following section.

**The  $\beta$ -Agostic  $\pi$ -Complex.** Attack of the olefin on the resting state  $\beta$ -8 leads in a very exothermic reaction ( $\Delta H = -37.1$  kJ/mol) to the formation of the  $\beta$ -agostic  $\pi$ -complex  $\beta$ -9 (Figure 2). The  $\pi$ -complex  $\beta$ -9 is virtually  $C_s$  symmetric with Zr, C $\alpha$ , C $\beta$ , H $\beta$ , C $_2$ , and C $_1$  being almost perfectly in a plane (Zr-C $\alpha$ -C $\beta$ -H $\beta$  = 2.7°; C $_1$ -Zr-C $\alpha$ -C $\beta$  = -0.1°). The structure is stabilized by a strong  $\beta$ -agostic interaction which is obvious from the short Zr-H $\beta$  (205.4 pm) and the long C $\beta$ -H $\beta$  (117.9 pm) distance. In going from the resting state  $\beta$ -8 to the  $\pi$ -complex  $\beta$ -9 the ethyl group has to move further out of the plane defined by the two centroids and the zirconium atom ( $\alpha = 66.6^\circ$ ) in order to make room for the incoming olefin. It has been shown that this process is facile.<sup>22,38</sup> The agostic hydrogen atom points toward C $_2$  of the complexed ethylene. The orientation of the hydrogen points to the possible H-exchange reaction will be discussed in section IV.

In the next section we investigate the rotation around Zr-C $\alpha$ , which is (i) a measure for the ease of movement out of the plane and (ii) a possible pathway for the transformation of the  $\beta$ -agostic  $\pi$ -complex to an  $\alpha$ -agostic  $\pi$ -complex.

**Rotation around Zr-C $\alpha$ .** The calculated profile for the rotation around Zr-C $\alpha$  is shown in Figure 3. The angle  $\theta$  corresponds to the torsional angle C $\beta$ -C $\alpha$ -Zr-midpoint (C $_2$ =C $_1$ ). From Figure 3 it is evident that at least in the beginning of the rotation hardly any energy is needed to move the methyl group out of the plane, thus this vibration should be highly excited. On the non-local level of theory a structure with  $\theta = 20^\circ$  is even 0.9 kJ/mol more stable than the LDA minimum structure ( $\theta = 0^\circ$ ). Only 1.2 kJ/mol are necessary for an out of plane angle of 30° and the 40° structure is 7.4 kJ/mol higher in energy than the zero-point structure. We conclude that the  $\pi$ -complex  $\beta$ -9 is a highly flexible structure, which spends only a very short time in the planar orientation depicted in Figure 3. (A more detailed discussion will be provided later.)

Rotation leads to the loss of the  $\beta$ -agostic interaction and simultaneously the C $\alpha$ -C $_2$  distance decreases slightly allowing the olefin to move away from the Cp rings. Notice that close to the transition state  $10^\ddagger$  no change in distance is observed. Thus  $10^\ddagger$  is the transition state for the rearrangement of the polymer chain from a  $\beta$ -agostic orientation to an  $\alpha$ -agostic

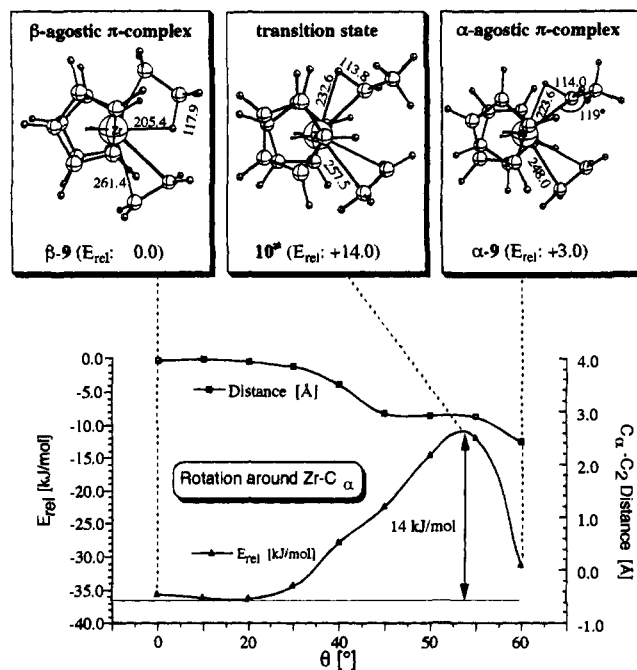


**Figure 3.** Profile for the rotation around Zr-C $\alpha$  and stationary points. The angle  $\theta$  corresponds to the torsional angle defined by C $\beta$ -C $\alpha$ -Zr-midpoint (C $_2$ =C $_1$ ); distances in pm.

$\pi$ -complex and *not* the transition state for the insertion process. The transition state  $10^\ddagger$  has an activation barrier of 14.0 kJ/mol relative to the  $\beta$ -agostic  $\pi$ -complex. In  $10^\ddagger$  the  $\beta$ -agostic interaction is broken, but the  $\alpha$ -agostic interaction has not yet formed (Zr-H $\alpha$  = 232.6 pm; C $\alpha$ -H $\alpha$  = 113.8 pm), although the Zr-C $\alpha$ -H $\alpha$  angle is already relatively small (100.9°). The C $\alpha$ -C $_2$  distance has decreased to 291.3 pm. Optimization of the next step ( $\theta = 60^\circ$ ) in the linear transit led directly to insertion and the formation of the product. Without constraining the C $\alpha$ -C $_2$  distance we were not able to locate further stationary points on the potential surface. Thus the reaction coordinate from this point on is better described by the C $\alpha$ -C $_2$  distance.

It is a known fact that LDA tends to overestimate weak interaction, such as  $\pi$ -bonding of an olefin or agostic interactions. This makes it necessary to check the validity of the NL/LDA approximation in this case. We thus reoptimized the  $\beta$ -agostic  $\pi$ -complex  $\beta$ -9, the transition state  $10^\ddagger$ , and the  $\alpha$ -agostic  $\pi$ -complex  $\alpha$ -9 at the non-local level of theory. The calculated activation barrier amounts to 22 kJ/mol as compared to 14 kJ/mol for the LDA geometry. The relative energy of the  $\alpha$ -agostic  $\pi$ -complex (+4.9 kJ/mol) compares well with the respective value at the local level of theory (+3.0 kJ/mol). Thus the agreement between NL/LDA and NL/NL energies is good and one might expect that the NL/LDA transition state bear an error for the activation barrier which is less than 10 kJ/mol. The main difference between local and non-local geometries is the expected longer Zr-olefin distance in the latter. The Zr-C $_{olefin}$  distance has increased from 261.4 to 282.1 pm in  $\beta$ -9, from 257.5 to 277.8 pm in  $10^\ddagger$ , and from 248.0 to 263.4 pm in  $\alpha$ -9. This agrees well with X-ray data by Wu *et al.*, who found a rather large range for the Zr-C $_{olefin}$  distances in Cp $_2$ Zr(OCMe $_2$ -CH $_2$ CH $_2$ CH=CH $_2$ )<sup>+</sup> (Zr-C $_{olefin,terminal}$  = 268 pm; Zr-C $_{olefin,internal}$  = 289 pm).<sup>58</sup> There are two conclusions which can be drawn from this: (i) already the agreement between the LDA geometries with experimental structures is good, and (ii) the small change in energy on going from a LDA to a NL structure

(58) Wu, Z.; Jordan, R. F.; Petersen, J. L. *J. Am. Chem. Soc.* **1995**, *117*, 5867.

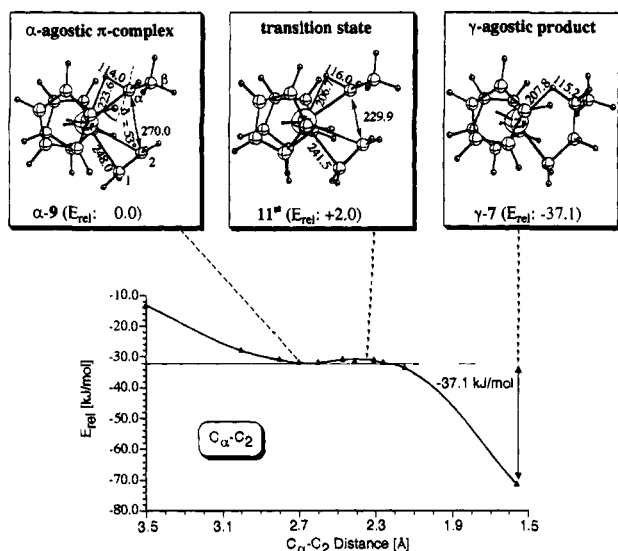


**Figure 4.** Stationary points and reaction profile for the frontside insertion; relative energies in kJ/mol, bond lengths in pm, angles in deg.

nically proves that the energy is only marginally influenced by a change in the Zr–olefin distance which means that the olefin is only loosely bound. Furthermore, it seems noteworthy that the already weak  $\alpha$ -agostic interaction in  $11^*$  disappeared at the non-local level (Zr–H = 288.9 pm; C–H = 110.3 pm), whereas the agostic interactions in  $\alpha$ - and  $\beta$ -9 are comparable to those at the local level. From these findings we conclude that non-local energies calculated for local geometries give a reasonable though lower estimate for the computationally much more demanding purely non-local values. Thus in the following we will restrict ourselves to the discussion of non-local energies based on local geometries. In the next section we will look at the insertion more closely.

**Insertion of the Olefin.** In this section we will discuss the insertion profile as obtained using the  $C_\alpha$ – $C_2$  distance as the reaction coordinate (Figure 4). From Figure 4 we can see that the  $\alpha$ -agostic  $\pi$ -complex  $\alpha$ -9 is located in a very shallow minimum and that the activation energy for the insertion from that point amounts to only 2.0 kJ/mol. There is virtually no activation barrier separating an  $\alpha$ -agostic  $\pi$ -complex and the product. This observation is in agreement with other MO studies by Woo *et al.*<sup>37,38</sup> as well as Weiss *et al.*,<sup>26</sup> who found similar reaction profiles for the insertion of ethylene into the methylbis(cyclopentadienyl)zirconium (titanium) cation: MP2 calculations yielded an activation barrier of 4 kJ/mol,<sup>26</sup> whereas the non-local DFT study gave a barrier of 3 kJ/mol.<sup>37,38</sup> The low activation barrier is further supported by a LDA-Car Parrinello investigation by Meier *et al.*,<sup>30</sup> which gave no insertion barrier.

In the following we shall describe the stationary points. The  $\alpha$ -agostic  $\pi$ -complex  $\alpha$ -9 has a remarkably large Zr– $C_\alpha$ – $C_\beta$  angle of  $135.2^\circ$ , which minimizes steric interactions between the Cp rings and the methyl group. At the same time,  $C_\alpha$  has tilted ( $\delta = 53^\circ$ ) so that interactions with the inserting olefin are possible. (The tilt angle  $\delta$  is defined as the angle between the local  $C_3$  axis of  $C_\alpha$  and the M– $C_\alpha$  bond vector.) The olefin is loosely bound ( $C_1$ – $C_2 = 135.0$  pm; Zr– $C_1 = 248.0$  pm) and the complex is asymmetric. The  $\alpha$ -agostic  $\pi$ -complex  $\alpha$ -9 is only 3 kJ/mol less stable than the corresponding  $\beta$ -agostic complex  $\beta$ -9, although the free  $\alpha$ -agostic resting state  $\alpha$ -8 is 47.0 kJ/mol higher in energy than  $\beta$ -8. This can be explained with reduced steric interactions in  $\alpha$ -9 as pointed out earlier. The transition state  $11^*$  closely resembles the  $\pi$ -complex  $\alpha$ -9,

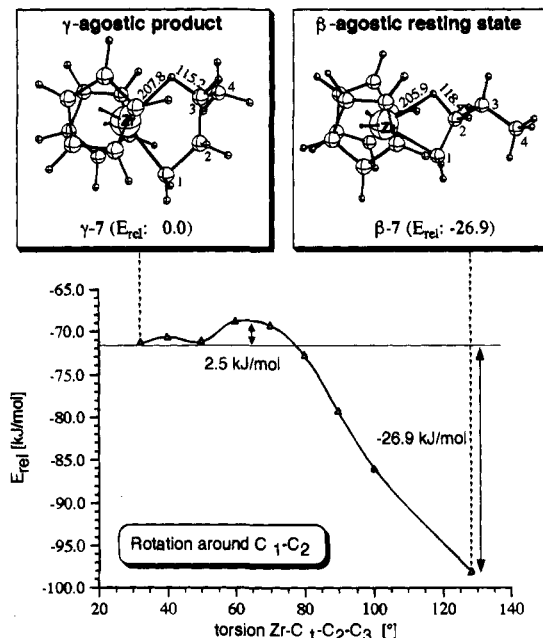


**Figure 5.** Stationary points and rotational profile for the reorientation of the product; energies in kJ/mol.

except that the  $C_\alpha$ – $C_2$  distance has decreased from 270.0 to 229.9 pm and that the olefin–carbon atoms are closer to the plane. The primary  $\gamma$ -agostic product is 34.2 kJ/mol more stable than the  $\beta$ -agostic  $\pi$ -complex  $\beta$ -9. Thus the reaction is very exothermic. In the product  $\gamma$ -7 steric interactions are minimized through a ring-tilt allowing an all-staggered orientation of the protons as well as the terminal methyl group.

**Reorientation of the Primary Product.** As pointed out earlier, the  $\gamma$ -agostic orientation of the product is not the most stable structure. In Figure 5 the profile of the rearrangement of  $\gamma$ -7 to the  $\beta$ -agostic resting state  $\beta$ -7, corresponding to a rotation around  $C_1$ – $C_2$ , is shown. From Figure 5 it becomes evident that the rotation is easy and the activation barrier amounts to only 2.5 kJ/mol. Thus we conclude that the product immediately rearranges to its most stable orientation after the insertion has taken place. The  $\beta$ -agostic structure  $\beta$ -7 is 26.9 kJ/mol more stable than the conformer  $\gamma$ -7. In  $\beta$ -7 a strong agostic interaction is present (Zr–H = 205.9 pm; C–H = 118.4 pm) and the chain end points away from the Cp rings. Steric interactions are small because of the large  $C_1$ – $C_2$ – $C_3$  angle of  $116.5^\circ$  putting the chain end away from the cyclopentadienyl ligands.  $\beta$ -7 resembles the starting structure  $\beta$ -8 except that the polymer chain is elongated by a  $C_2$  unit. Thus we now have the complete reaction profile from resting state to resting state in hand.

**The Complete Profile from  $\beta$ -Agostic Resting State to  $\beta$ -Agostic Resting state.** In Figure 6 the three profiles given in Figures 3, 4, and 5 are combined. From Figure 6 it is obvious that the experimentally observed propagation barrier corresponds to the rotation around Zr– $C_\alpha$  prior to insertion. The calculated barrier of 14 kJ/mol is slightly smaller than the experimental estimate of 25–32 kJ/mol.<sup>40–43</sup> It can be assumed that inclusion of solvent effects will raise the free energy of activation because of friction. From the  $\alpha$ -agostic  $\pi$ -complex,  $\alpha$ -9, the reaction proceeds virtually without any further activation barriers or intermediates to the  $\beta$ -agostic product  $\beta$ -7. The calculated activation barrier for the *insertion* is 2.0 kJ/mol, the barrier for the product *rearrangement* amounts to 2.5 kJ/mol. A look at the change in  $C_2$ – $C_\alpha$  bond distance and angle  $\theta$  reveals that both are changed during the rotation. This leads to the conclusion that rotation and insertion take place in a concerted reaction.

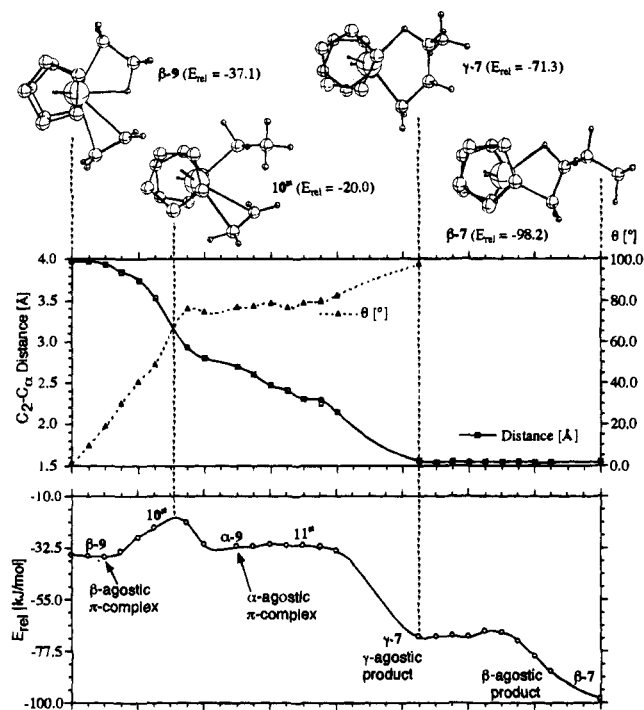


**Figure 6.** Complete propagation profile. The angle  $\theta$  corresponds to the torsional angle defined by  $C_\beta-C_\alpha-Zr$ -midpoint ( $C_2=C_1$ ); energies in kJ/mol.

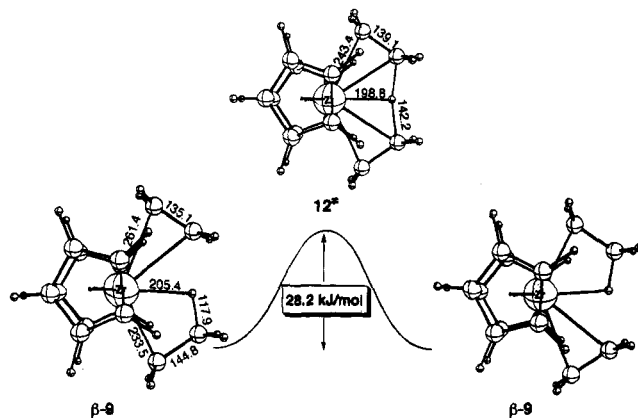


**Figure 7.** Stationary points and schematic reaction profile for the H-exchange;<sup>44</sup> relative energy in kJ/mol, bond lengths in pm, angles in deg.

The overall reaction is very exothermic relative to both the isolated molecules ( $-98.2$  kJ/mol) and the  $\beta$ -agostic  $\pi$ -complex  $\alpha$ -9 ( $-61.1$  kJ/mol), which is in line with an estimate of  $-82$  kJ/mol based on the formation of two C-C single bonds (BDE = 348 kJ/mol) from one C=C double bond (BDE = 614 kJ/mol).<sup>59</sup>

#### IV. Comparison with Other Reactions

**Comparison with the H-Exchange Reaction (Chain Termination).** Comparison of the presented propagation barrier with the earlier published<sup>44</sup> barrier for the chain termination via hydrogen exchange shows no clear preference for either of the reactions. The H-exchange reaction starts from the same ( $\beta$ -agostic)  $\pi$ -complex  $\beta$ -9 as the insertion and has an activation barrier of 28.2 kJ/mol (Figure 7) whereas the calculated propagation barrier is 14.0 kJ/mol. Applying Maxwell-Boltzmann statistics<sup>57</sup> to this energy difference yields ca. 300

insertions per chain termination. Thus, without consideration of other effects, molecular weights of ca. 8000 g/mol should be expected, which clearly contradicts experimental results, where molecular weights larger than 100 000 g/mol were often obtained.<sup>4</sup>

What is the reason for the strong preference of insertion over H-exchange? From Figure 3 we have concluded that the  $\pi$ -complex  $\beta$ -9 is extremely flexible and that the out-of-plane vibrational mode is highly excited. Thus, the ethyl group in the  $\pi$ -complex has only a low probability to be exactly in the plane; most of the time it will be out of the plane. A prerequisite for the H-exchange reaction, however, is that both the olefin and the ethyl group are in a plane: The transition state for hydrogen exchange,  $12^\ddagger$ , is almost exactly planar ( $C_1-Zr-C_\alpha-C_\beta = 0.1^\circ$ ;  $Zr-C_\alpha-C_\beta-H = 1^\circ$ ). The rotation insertion on the other hand should be favored by a highly mobile  $\pi$ -complex, since the rotational mode, which basically corresponds to the reaction mode, would already be highly occupied. Both facts are supported by the calculated vibrational frequencies for the respective modes.

A frequency analysis of the  $\beta$ -agostic  $\pi$ -complex,  $\beta$ -9, reveals that the mode corresponding to the out-of-plane vibration of the  $\beta$ -methyl group has a vibrational frequency of only 119  $\text{cm}^{-1}$ , which means that the methyl group is extremely mobile and has a strong tendency to rotate out of the plane. The  $C_\beta-H_\beta$  stretch vibration (2121  $\text{cm}^{-1}$ ), on the other hand, although at lower wavenumbers than a normal C-H stretch, is much higher in energy. This leads to the conclusion that a rotation around  $Zr-C_\alpha$  should have a higher probability than the H-transfer (which corresponds to the C-H stretch vibration).

Entropic considerations point in the same direction. The transition state for the H-exchange is compact and the degrees of freedom related to the movement of the hydrogen as well as the olefin and the chain end are considerably frozen. The rotation of the ethyl group on the other hand does not suffer from similar restrictions, because the  $\beta$ -agostic interaction is broken and the  $\alpha$ -agostic has not yet formed. Thus, no coordinates except the reaction coordinate are "frozen". This should lead to a more negative activation entropy for the H-exchange than for the rotation, which will increase the relative free energy of activation and make the chain termination reaction less favorable. In order to further corroborate the effect of dynamics on the reaction barriers, we carried out a thermal analysis based on the frequency calculations.

Table 1 summarizes the entropy and energy contributions at room temperature. All quantities were calculated according to standard textbook procedures.<sup>57</sup> The imaginary frequencies for the transition states were neglected in the calculation of vibrational entropy and energy.  $\Delta S$ ,  $\Delta H$ , and  $\Delta G$  are given with respect to the  $\pi$ -complex  $\beta$ -9.

A striking feature of the transition state for the rotation is that it has a positive entropy of activation ( $\Delta S^\ddagger = +18.3$  J/(mol·K)), mainly due to an increased vibrational entropy ( $\Delta S_{\text{vib}} = +17.7$  J/(mol·K)). This is understandable, if one recalls that the transition state  $10^\ddagger$  does not have any agostic hydrogen atoms, whereas the  $\pi$ -complex  $\beta$ -9 exhibits a strong  $\beta$ -agostic interaction, which in this case increases the entropy of the transition state relative to the  $\pi$ -complex. On the other hand, the transition state for the H-exchange reaction  $12^\ddagger$  shows a slightly negative entropy of activation ( $\Delta S^\ddagger = -4.5$  J/(mol·K)), which is in agreement with our earlier assumption that the H-exchange reaction takes place via a highly ordered transition state. A thorough analysis of the vibrations reveals that there are low-energy vibrations (symmetric and asymmetric) for the out-of-plane vibrations of the two C2 units. These account for

(59) Darwent, B. d. B. *Bond Dissociation Energies in Simple Molecules*; NSRDS-NBS 31: Washington, D.C., 1970.

**Table 1.** Thermodynamic Data of the Barriers for Propagation, H-Exchange, and Backside Insertion with the  $\beta$ -Agostic  $\pi$ -Complex  $\beta$ -9 as a Reference

	<b>10<sup>‡</sup></b> rotation transition state	<b>12<sup>‡</sup></b> H-exchange transition state	<b>13</b> backside $\pi$ -complex	<b>14<sup>‡</sup></b> backside insertion transition state <sup>a</sup>
$\nu_{MAG}$ [cm <sup>-1</sup> ]	101i	490i		245i
$\Delta S_{trans}$ [J/(mol·K)]	0.00	0.00	0.00	0.00 (0.00)
$\Delta S_{rot}$ [J/(mol·K)]	0.61	-0.09	0.04	-0.18 (-0.22)
$\Delta S_{vib}$ [J/(mol·K)]	17.71	-4.40	-2.56	-18.48 (-15.92)
$\Delta S_{tot}$ [J/(mol·K)]	<b>18.32</b>	<b>-4.49</b>	<b>-2.53</b>	<b>-18.66 (-16.13)</b>
$\Delta H_{trans}$ [kJ/mol]	0.00	0.00	0.00	0.00 (0.00)
$\Delta H_{rot}$ [kJ/mol]	0.00	0.00	0.00	0.00 (0.00)
$\Delta H_{vib}$ [kJ/mol]	2.11	-1.26	-0.34	-2.47 (-2.13)
$\Delta H_0$ [kJ/mol]	-10.36	-4.10	0.51	1.99 (1.48)
$\Delta H_{elec}$ [kJ/mol]	14.05	28.22	-6.77	21.58 (28.35)
$\Delta H_{tot}$ [kJ/mol]	<b>5.80</b>	<b>22.86</b>	<b>-6.60</b>	<b>21.10 (27.70)</b>
$\Delta G$ [kJ/mol]	<b>0.34</b>	<b>24.20</b>	<b>-5.85</b>	<b>26.66 (32.51)</b>
<b>298.15 K</b>				

<sup>a</sup> Values in parentheses with respect to 13.

the relatively small negative activation entropy. For the rotation transition state, **10<sup>‡</sup>**, zero-point energy ( $\Delta H_0$ ) points in the same direction as the entropy. This greatly reduces the electronic barrier of activation ( $\Delta H_{elec} = +14.0$  kJ/mol) at 0 K to a negligible free energy of activation ( $\Delta G^\ddagger = +0.34$  kJ/mol at 298.15 K) for **10<sup>‡</sup>**. At this point one should recall that the process is studied in vacuo and that it can be assumed that inclusion of solvent effects will raise the free energy of activation due to solvent friction. In the case of the H-exchange reaction the effects of zero-point energy and vibrational energy are partially canceled by the activation entropy. The electronic barrier ( $\Delta H_{elec} = +28.2$  kJ/mol) is only slightly reduced to a free energy of activation ( $\Delta G^\ddagger = +24.2$  kJ/mol). Maxwell-Boltzmann statistics now yield a ratio of 15000/1 (rotation/chain termination) taking the  $\pi$ -complex as the reference point for the frontside insertion, which is in much better agreement with the experiment than the ratio based only on the electronic barriers.

We therefore conclude that from a dynamics point of view the H-exchange reaction is very unlikely, whereas the propagation will be favored when vibrations are taken into account. We are currently undertaking a nonlocal Car-Parrinello dynamics study in order to further corroborate the conclusions drawn in this section.<sup>60</sup>

**Comparison with the Backside Insertion.** Another reaction of the cationic ethylzirconocene  $\beta$ -8 with ethylene is the backside insertion (Figure 8)<sup>44</sup>. The olefin approaches the resting state from the backside and forms the backside  $\pi$ -complex **13**, which is 6.8 kJ/mol more stable than the  $\beta$ -agostic frontside complex  $\beta$ -9. The ethyl group has moved to the other side ( $\alpha = -24.6^\circ$ ) in order to accommodate the olefin. **13** shows a strong  $\beta$ -agostic interaction (Zr-H $_\beta$  = 204.5 pm; C $_\beta$ -H $_\beta$  = 116.4 pm) and the complex is practically C $_s$  symmetric. The transition state **14<sup>‡</sup>** is 28.4 kJ/mol higher in energy and is advanced considering a C $_2$ -C $_\alpha$  distance of only 202.2 pm.

What is the effect of the dynamics on the reaction barrier for this process? From Table 1 we can see that the transition state has a strongly negative activation entropy ( $\Delta S^\ddagger = -16.1$  J/(mol·K)) relative to the backside  $\pi$ -complex **13**. The reason for this large negative  $\Delta S^\ddagger$  is the late and compact transition state. Furthermore, the out-of-plane rotation of the ethyl group is hindered because the  $\beta$ -methyl-group is pointing toward the Cp rings. In the rotational transition state **10<sup>‡</sup>** the olefin can almost freely rotate and translate with respect to the metallocene, which leads to an increase in entropy because of the additional

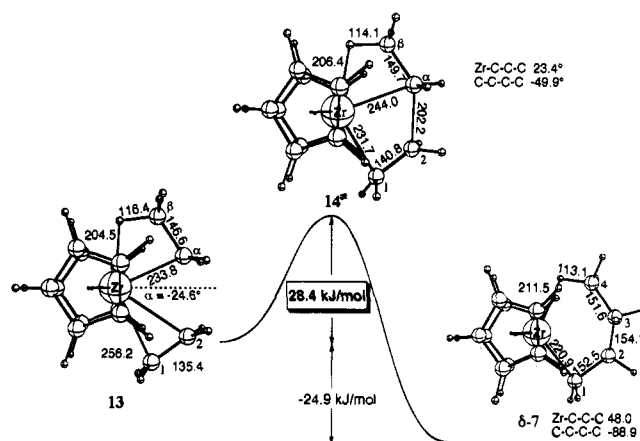


**Figure 8.** Stationary points and schematic reaction profile for the backside insertion;<sup>44</sup> relative energy in kJ/mol, bond lengths in pm, angles in deg.  $\alpha$  is the out-of-plane angle of the  $\alpha$ -carbon atom with respect to the centroid-Zr-centroid plane

loss of an agostic interaction, whereas in the backside insertion transition state the olefin is strongly bonded, i.e. the six degrees of freedom corresponding to rotation and translation of the olefin are almost completely lost giving rise to a large negative entropy of activation. The change in zero-point and vibrational energy at 298.15 K on the other hand is small, which in total increases the electronic barrier ( $\Delta H_{elec} = +28.4$  kJ/mol relative to **13**) to a free energy of activation of  $\Delta G^\ddagger = 32.5$  kJ/mol (relative **13**). Hence, taking entropic effects into account the backside insertion (which might lead to stereo defects as pointed out earlier<sup>44</sup>) becomes less likely if compared to the rotation around Zr-C $_\alpha$ .

## V. Conclusion

In the present paper we investigated the reaction of  $Cp_2ZrEt^+$  with ethylene. We studied the whole propagation profile from one  $\beta$ -agostic resting state to the next resting state. This was necessary, since earlier investigations showed (i) the importance and the stability of  $\beta$ -agostic structures and (ii) a low barrier (2–4 kJ/mol)<sup>26,37,38,44</sup> for the insertion into an  $\alpha$ -agostic structure which is not in line with experimental estimates of the propagation barrier (28–40 kJ/mol).<sup>40–43</sup> It was therefore concluded that the rearrangement of the polymer chain prior to or after the insertion has to account for the propagation barrier.<sup>44,37</sup>

The reaction of  $Cp_2Et^+$  with ethylene starts with the formation of a  $\beta$ -agostic  $\pi$ -complex  $\beta$ -9 in an exothermic reaction ( $\Delta H$

(60) Margl, P.; Lohrenz, J. C. W.; Ziegler, T. *J. Am. Chem. Soc.* **1995**, submitted.



= -37.1 kJ/mol). It can react in two ways: (i) rotation around the Zr-C $\alpha$  bond can take place leading to an  $\alpha$ -agostic complex and (ii) H-transfer to the olefin is possible, which would lead to chain termination.

The rotation around Zr-C $\alpha$  is facile ( $\Delta H^\ddagger = 14.1$  kJ/mol) and connects the  $\beta$ -agostic  $\pi$ -complex  $\beta$ -9 with the corresponding  $\alpha$ -agostic structure  $\alpha$ -9, from which insertion is known to take place virtually without barrier ( $\Delta H^\ddagger = 2.0$  kJ/mol).<sup>44</sup> In the transition state  $10^\ddagger$  the  $\beta$ -agostic interaction is lost and an  $\alpha$ -agostic bond has not yet formed, although the Zr-C $\alpha$ -H $\alpha$  angle is already small.

It was shown that the rotation is further facilitated by the high mobility of the ethyl group in  $\beta$ -9: The out-of-plane vibration has a very low frequency (119 cm<sup>-1</sup>). This is reflected in a positive activation entropy ( $\Delta S^\ddagger = +18.3$  J/(mol·K)) and a large change in zero-point energy ( $\Delta H_0 = -10.4$  kJ/mol) on going from the  $\pi$ -complex to the transition state, which leads to a small free energy of activation ( $\Delta G^\ddagger = +0.34$  kJ/mol). Thus the rotation is favorable but has an electronic barrier of 14 kJ/mol.

We assume that the small activation energy for the rotation is slightly underestimated because of the relatively small size of the ethyl group. One can expect that during the polymerization a larger polymer chain will be less mobile, thus reducing the activation entropy as well as increasing the zero-point energy. Second, friction due to the solvent will have a similar effect. In the case of very large polymer chains it can be proposed that the metallocene has to rotate around the chain end, which will further decrease the entropy of activation. We conclude that the calculated barrier is a lower limit for the process.

Once the  $\alpha$ -agostic  $\pi$ -complex  $\alpha$ -9 has formed the reaction proceeds without any notable barriers to the  $\beta$ -agostic product  $\beta$ -7. Insertion takes place with an activation barrier of only 2 kJ/mol yielding a  $\gamma$ -agostic primary product  $\gamma$ -7 ( $\Delta H = -34.2$  kJ/mol), which then rearranges through a rotation around the C $\alpha$ -C $\beta$  bond ( $\Delta H^\ddagger = 2.5$  kJ/mol) to form the  $\beta$ -agostic resting state in an exothermic reaction ( $\Delta H = -26.9$  kJ/mol). Starting from the isolated ethylene and Cp<sub>2</sub>Zr<sup>+</sup>-Et the reaction is exothermic by -98.2 kJ/mol, which agrees well with the expected exothermicity based on bond dissociation energies (-82 kJ/mol).<sup>59</sup> A comparison of the three involved reaction steps (rotation prior to insertion, insertion, and product rearrangement) shows clearly that the propagation barrier corresponds to the rearrangement of the  $\pi$ -complex prior to insertion. It can be assumed that rotation and insertion take place in a concerted process (Figure 6).

Other high-level quantum mechanical studies support this interpretation since they found only low activation barriers (2-4 kJ/mol)<sup>26,38,44</sup> for the insertion of ethylene into metallocene cations (M = Ti, Zr).

As pointed out earlier, the  $\beta$ -agostic  $\pi$ -complex can lead to hydrogen exchange. This reaction has been studied earlier in detail<sup>35,44</sup> and leads to chain termination. A prerequisite for the H-exchange is the planar arrangement of both the ethyl group and the ethylene. The hydrogen is transferred with an activation barrier of 28.2 kJ/mol in an almost planar C<sub>2</sub>-symmetric

transition state  $12^\ddagger$ . Calculation of the Maxwell-Boltzmann distribution based on the difference between the activation barriers for rotation and H-exchange yields a ratio of 300/1, i.e. only oligomers should be obtained. The rigidity of the hydrogen exchange transition state  $12^\ddagger$ , however, is reflected in a negative entropy of activation and only minor changes in zero-point energy and vibrational energy, yielding a positive free energy of activation ( $\Delta G^\ddagger = 20.1$  kJ/mol) compared to  $\Delta G^\ddagger = -10.0$  kJ/mol for the rotation  $10^\ddagger$ . This greatly changes the expected reaction ratio to 15000/1 in favor of the propagation, which is in excellent agreement with the large experimentally observed molecular weights well above 100 000 g/mol.<sup>4</sup> The latter considerations nicely show the importance of dynamical effects and the corresponding large changes to the reaction barriers in the case of the metallocene systems.

Attack at the backside of the resting state was considered to be an alternative reaction path. The backside  $\pi$ -complex  $13$  is slightly more stable (-5.2 kJ/mol) than the  $\beta$ -agostic frontside  $\pi$ -complex  $\beta$ -9 and exhibits a strong  $\beta$ -agostic interaction (Zr-H $\beta$  = 204.5 pm; C $\beta$ -H $\beta$  = 116.4 pm). The electronic barrier for the insertion is relatively high ( $\Delta H^\ddagger = +28.4$  kJ/mol) and there is a strongly negative entropy of activation ( $\Delta S^\ddagger = -16.1$  J/(mol·K)), due to a very compact transition state  $14^\ddagger$  which is late on the reaction coordinate (C<sub>2</sub>-C $\alpha$  = 202.2 pm). This leads to a free energy of activation of +32.5 kJ/mol, making this reaction unlikely if compared to the negative activation barrier for the frontside propagation (rotation). It has been shown that the backside insertion mechanism is not in line with the experimentally observed site control in the case of the syndio-selective polymerization since it should lead to isotactic polymer.<sup>44</sup> We assume that backside insertion results in misinsertions for this case.

Taking all three reactions studied in this paper together, one can draw the following conclusions: (i) The resting state between two insertions is a  $\beta$ -agostic structure. (ii) Frontside insertion is possible and has a low barrier. (iii) The propagation barrier results from the rearrangement of the  $\beta$ -agostic  $\pi$ -complex to an  $\alpha$ -agostic complex prior to insertion. (iv) The latter process has a small electronic barrier. (v) The formation of the  $\beta$ -agostic resting state from the primary  $\gamma$ -agostic product is facile and exothermic. (vi) H-exchange, i.e. chain termination, from the  $\beta$ -agostic  $\pi$ -complex has a moderate electronic activation barrier but has a low probability because of the high flexibility of the  $\pi$ -complex. (vii) Backside insertion, although feasible, has a higher activation barrier than the frontside propagation, and is entropically disfavored.

**Acknowledgment.** This investigation was supported by the Natural Science and Engineering Research Council of Canada (NSERC) as well as the donors of the Petroleum Research Fund, administered by the American Chemical Society (ACS-PRF No. 27023-AC3). J. C. W. Lohrenz wishes to thank the Fond der Chemischen Industrie who supported this work with a Liebig-Stipendium. T.K.W. wishes to thank the Izaak Walton Killam Memorial Foundation.

JA951885V